International Journal of Applied Science and Engineering
2011. 9, 4: 223-239

Preparation of $MnFe_2O_4$ Nanoceramic Particles by Soft Chemical Routes

Susan Sam and A. Samson Nesaraj *

Department of Chemistry, Karunya University, Karunya Institute of Technology and Sciences Karunya Nagar, Coimbatore -641 114, Tamil Nadu, India.

Abstract: $MnFe_2O_4$ is one of the most common spinel ferrites and its nanoparticles have found applications in various applications. In this paper, we report the preparation of $MnFe_2O_4$ nanocrystalline spinel particles by different techniques viz., low temperature combustion technique using urea, glycine and glucose as fuels and chemical-precipitation method. The resulting powder was characterized by XRD, particle size analysis and SEM. The XRD pattern confirmed the presence of cubic phase in all the samples. The particle size data of the powder prepared with chemical precipitation route revealed that 42.8 % of particles lie below 229 nm. The surface microstructure elucidation by SEM also confirmed the presence of uniform sized nanoparticles in the sample prepared by co-precipitation method.

Keywords: $MnFe_2O_4$ spinel; preparation; combustion; chemical precipitation; characterization

1. Introduction

Recently, interest in the use of magnetic nanoparticles (MNPs) has increased due to their unique multifunctional properties. Magnetic materials, in nanosized form, are useful for a variety of applications such as biomedical applications, magnetic storage, ferrofluids, etc. Manganese ferrite ($MnFe_2O_4$) is a well-studied spinel ferrite that has low magnetic anisotropy at room temperature (K_1= −33 X 10^3 erg/cm^3 or $H_u = 2|K_1|/M_S$ = 175 Oe at 20 °C) arising from the low magneto crystalline anisotropy energy common to cubic magnetic structures [1]. Soft ferrites like $MnFe_2O_4$, owing to their simple preparation and good magnetic characteristics, are frequently applied in microwave devices, computer memory chips, magnetic recording media, radio frequency coil fabrication, transformer cores, rod antennas and many branches of telecommunication and electronic engineering. Also, these magnetic nanoparticles have been recognized for potential use in magnetic hyperthermia, referring to the introduction of ferromagnetic or super paramagnetic particles into the tumor tissue [2]. Recently, it was found that $MnFe_2O_4$ magnetic nano particles were effectively used an excellent adsorbent for the removal of the azo dye Acid Red B (ARB) from water [3]. Manganese ferrites belong to a group of soft ferrite materials characterized by high magnetic permeability and low losses. Previously, it was found that 80% of Mn occupies the A sites and 20% may go to the B sites, which makes it a partially inverse spinel [4].

Amighian et al. [5] synthesized $MnFe_2O_4$

* Corresponding author; e-mail: drsamson@karunya.edu *Accepted for Publication: September15, 2011*

via co-precipitation method using aqueous solution of starting materials ($FeSO_4.7H_2O$ and $MnSO_4.H_2O$) with precipitant NaOH. Teresa Valdes-Solis et al. [6] synthesized spinel ferrite $MnFe_2O_4$ by means of a nanocasting technique using a low cost mesoporous silica gel as hard template. The magnetic templates of <10 nm diameter and with a surface area around 100 m^2gm^{-1} were tested as a heterogeneous Fenton catalyst for the decomposition of hydrogen peroxide under neutral and basic conditions. Mishra et al. [7] synthesized nanostructured manganese ferrites with diameters in the range of 45-30 nm were synthesized by Ti^{4+} ion doping, using conventional solid-state reaction route. Rashad et al. [8] produced $MnFe_2O_4$ powders from low grade manganese ore after leaching of the ore in sulphuric acid and hydrogen peroxide. Yang et al. [9] reported a thermal decomposition approach to the synthesis of water-soluble super paramagnetic manganese ferrite ($MnFe_2O_4$) nanoparticles (NPs) for magnetic resonance (MR) imaging applications. In this approach, tetra ethylene glycol was utilized as a coordination and stabilization agent. The formed NPs had a diameter of 7 nm with a narrow size distribution, and were super paramagnetic with a saturated magnetization (Ms) of 39 emu/g.

Choi et al. [10] prepared $Mn_{(1-x)}Co_xFe_2O_4$ (where x= 0.0, 0.5, 1.0) materials by the high-temperature thermal decomposition method and studied for its unique magnetic phenomena of magnetic nanoparticles. The crystal structure is found to be an inverse cubic spinel with a space group of Fd-3m. Rucha et al. [11] synthesized $Mn_{0.5}Zn_{0.5}Fe_2O_4$ ferrite nanoparticles with tunable curie temperature and saturation magnetization using hydrothermal co-precipitation method. Iyer et al. [12] synthesized nanosized $Mn_{(1-x)}Zn_xFe_2O_4$ (where x= 0, 0.1, 0.3, 0.5, 0.6, 0.7, 0.9) mixed ferrites samples of particle size less than 12 nm using co-precipitation method by doping Zn^{2+} ion impurities. Deraz and Shaban [13] synthesized single domain manganese ferrite nanoparticles with narrow particle size distribution using the combustion technique. Influence of fuel ratios on the as prepared powders were characterized.

The fuel to cations ratio of 2.67 gives better yield in the formation of nanocrystalline Mn ferrite and single domain particles with a narrow range of size distribution. Ju et al. [14] have prepared $MnFe_2O_4$ spinel by electrospinning process they reported the structure of this material as cubic[3]. The structure of nano-crystalline $MnFe_2O_4$ was determined and refined with electron powder diffraction data employing the Rietveld refinement technique. The final structure was refined in space group Fd-3m (# 227) with lattice parameters a= 8.3413(7) Å [15]. From the above literature, it was clear that research efforts are now-a-days focussed towards synthesizing $MnFe_2O_4$ based ceramic materials for different applications. The present work is one such effort to synthesize $MnFe_2O_4$ particles by different soft chemistry methodologies and to study their physical properties.

2. Materials and Methods

2.1. Preparation of $MnFe_2O_4$ by combustion technique

The $MnFe_2O_4$ particles are prepared by the combustion synthesis process using urea / glycine / glucose as a fuels. The chemicals used in the preparative method are: $Mn(NO_3)_2.6H_2O$ (Loba Chemie, India, 97%), $Fe(NO_3)_3.9H_2O$ (Fischer Scientific, India, 98%), NH_2-CO-NH_2 (urea) (Merck, India, 99.5%) / NH_2-CH_2COOH (Fischer Scientific, India, 98.5%) (glycine) / $C_6H_{12}O_6$ (Fischer Scientific, India, 99%) (glucose) .

The combustion synthesis process involves the combustion of saturated aqueous solution containing stoichiometric quantities of the corresponding nitrates (oxidizers) and urea (NH_2-CO-NH_2) / glycine (NH_2-CH_2COOH) / glucose ($C_6H_{12}O_6$) fuel. The appropriate

quantities of the precursor salts were weighed accurately, taken in silica crucible and dissolved in triple distilled water. Calculated amount of fuel (urea / glycine / glucose) was added to the above solution with continuous stirring and homogenized well. The oxidizer: fuel ratio was calculated based on oxidizing (O) and fuel (F) valencies of the reactants keeping O/F =1 as reported [16, 17].

The aqueous redox solution containing metal nitrates and glycine when introduced into a muffle furnace [Model: Toshibha, India] preheated to 550 ^oC, boils, froths, ignites and catches fire (temperature 1100 ± 100 ^oC). At this higher temperature, the metal nitrates decompose to metal oxides and oxides of nitrogen and hence act as oxidizer for further combustion, which leads to a voluminous, foamy combustion residue in less than 5 minutes. The flame persisted for about 1 minute. The foam was then lightly ground in silica basin with porcelain pestle to obtain fine powders. The procedure is explained in the schematic (Figure 1). The stoichiometric proportion of precursor materials used for the synthesis of $MnFe_2O_4$ particles is indicated in Table 1.

Table 1. Stoichiometric proportion of the precursor materials used for the synthesis of $MnFe_2O_4$ powder

Weight of $Mn(NO_3)_2$ (g)	Weight of $Fe(NO_3)_3$ (g)	Weight of urea (g)	Weight of glycine (g)	Weight of glucose (g)
2.87	8.08	5	--	--
2.87	8.08	--	5	--
2.87	8.08	--	--	3.0

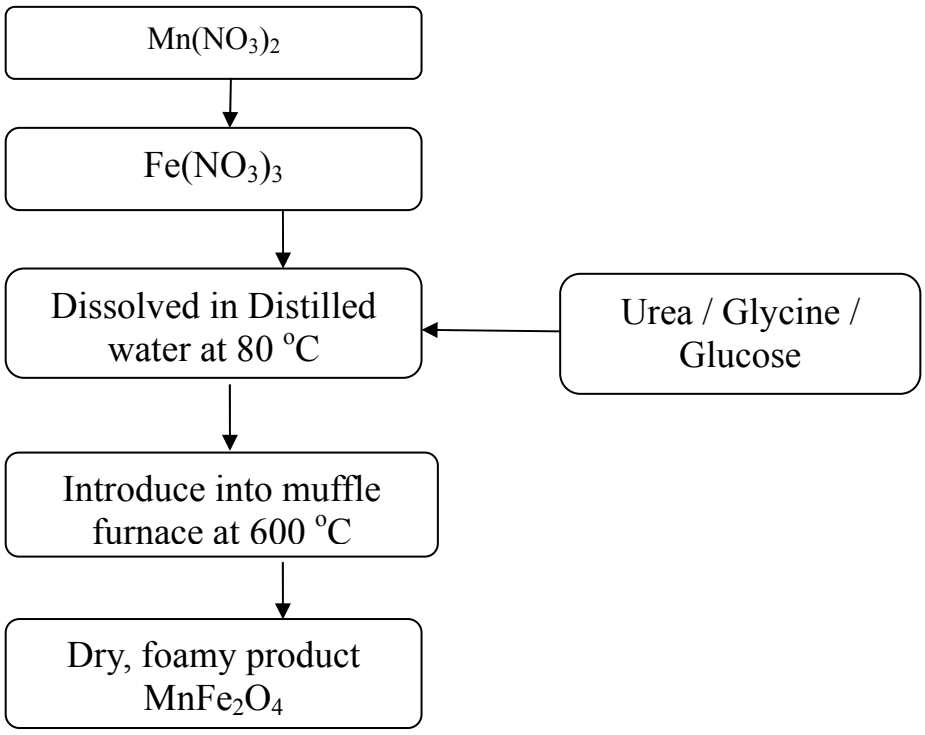

Figure 1. Flow chart to prepare $MnFe_2O_4$ particles by combustion technique using urea / glycine / glucose as fuels

The stoichiometric redox reactions between metal nitrates and urea or glycine or glucose to produce $MnFe_2O_4$ particles can be represented by the following theoretical equations:

To prepare $MnFe_2O_4$ by combustion technique with urea as a fuel:

$Mn(NO_3)_2 + 2\ Fe(NO_3)_3 + 6.66\ NH_2CONH_2 \rightarrow MnFe_2O_4 + 6.66\ CO_2 + 10.66\ N_2 + 13.32\ H_2O$

To prepare $MnFe_2O_4$ by combustion technique with glycine as a fuel:

$Mn(NO_3)_2 + 2\ Fe(NO_3)_3 + 4.44\ NH_2CH_2COOH \rightarrow MnFe_2O_4 + 8.88\ CO_2 + 6.22\ N_2 + 11.1\ H_2O$

To prepare $MnFe_2O_4$ by combustion technique with glucose as a fuel:

$Mn(NO_3)_2 + 2\ Fe(NO_3)_3 + 1.66\ C_6H_{12}O_6 \rightarrow MnFe_2O_4 + 9.96\ CO_2 + 4\ N_2 + 9.96\ H_2O + 0.04\ O_2$

The as-synthesized powder was carried out in clean alumina crucibles and calcined in air at 800 ^oC for 3 hours to remove the deposited carbon and the unreacted organic residues and to get a compound of pure phase [18].

2.2. Preparation of $MnFe_2O_4$ by co-precipitation method

High purity $MnSO_4.H_2O$ (Fischer Scientific, India, 99%), $FeSO_4.7H_2O$ (Fischer Scientific, India, 99%) and sodium hydroxide (Merck, India, 98%) were used in the preparation of $MnFe_2O_4$ nanoparticles. Initially, stoichiometric compositions of $MnSO_4$, $FeSO_4$ and sodium hydroxide were prepared separately in a 100 ml standard measuring flask using distilled water. Initially, $MnSO_4$ solution was added drop wise into the solution of alkali taken in 500 ml beaker. Immediately, $FeSO_4$ solution was added to the above solution. They were mixed perfectly by a magnetic stirring apparatus (1000 rpm) [Model – 2 MLH Remi, India] at room temperature for 1 hour. The resultant green coloured precipitate (mixture of $Mn(OH)_2 + Fe(OH)_2$) was filtered, and then washed with deionized water and ethanol for 5 – 10 times and was dried at 50 – 100^o C in an air oven [Model – Cryo Tech Hot Air Oven, India] for 24 hours. Then, the calcination was carried out at 300 ^oC, 500 ^oC, 600 ^oC and 800 ^oC for 2 hours each in a muffle furnace [Model: Toshibha, India]. During calcination at high temperature, oxygen deficient $MnFe_2O_4$was formed as per the following theoretical equation. Figure 2 shows a schematic illustration of the synthesis method. Main reactions occur during the experimental procedure can be written briefly as follows:

$4NaOH_{(s)} \rightarrow 4Na^+_{(aq)} + 4OH^-_{(aq)},$

$MnSO_4.H_2O_{(s)} \rightarrow Mn^{2+}_{(aq)} + SO_4^{2-}{}_{(aq)} + H_2O_{(aq)},$

$2FeSO_4.7H_2O_{(s)} \rightarrow 2Fe^{2+}_{(aq)} + 2SO_4^{2-}{}_{(aq)} + 14H_2O_{(aq)},$

$Mn^{2+} + 2OH^-_{(aq)} + xH_2O_{(aq)} \rightarrow Mn(OH)_2.xH_2O_{(s)}\downarrow,$

$2Fe^{2+}_{(aq)} + 4OH^-_{(aq)} + xH_2O_{(aq)} \rightarrow 2\ Fe(OH)_2 . xH_2O_{(s)}\downarrow,$

$$Mn(OH)_2.xH_2O_{(s)} + 2Fe(OH)_2 . x\ H_2O_{(s)} \xrightarrow{50\text{-}100^oC} Mn(OH)_{2(s)} + 2Fe(OH)_{2\ (s)} + xH_2O_{(g)}\uparrow,$$

$$Mn(OH)_{2(s)} + 2Fe(OH)_{2\ (s)} \xrightarrow{800^oC} MnFe_2O_{4-\delta(s)} + 3\ H_2O_{(g)}\uparrow.$$

2.3. Characterization of $MnFe_2O_4$

The powder XRD study was carried out using a Shimadzu XRD6000 X-ray diffractometer using CuKα radiation. The crystallite sizes of the $MnFe_2O_4$ were calculated by Scherrer's formula. The particle size of the powder was measured using a Malvern Particle Size Analyzer using triple distilled water as medium. The morphology of the particles was studied by means of JEOL Model JSM-6360 scanning electron microscope.

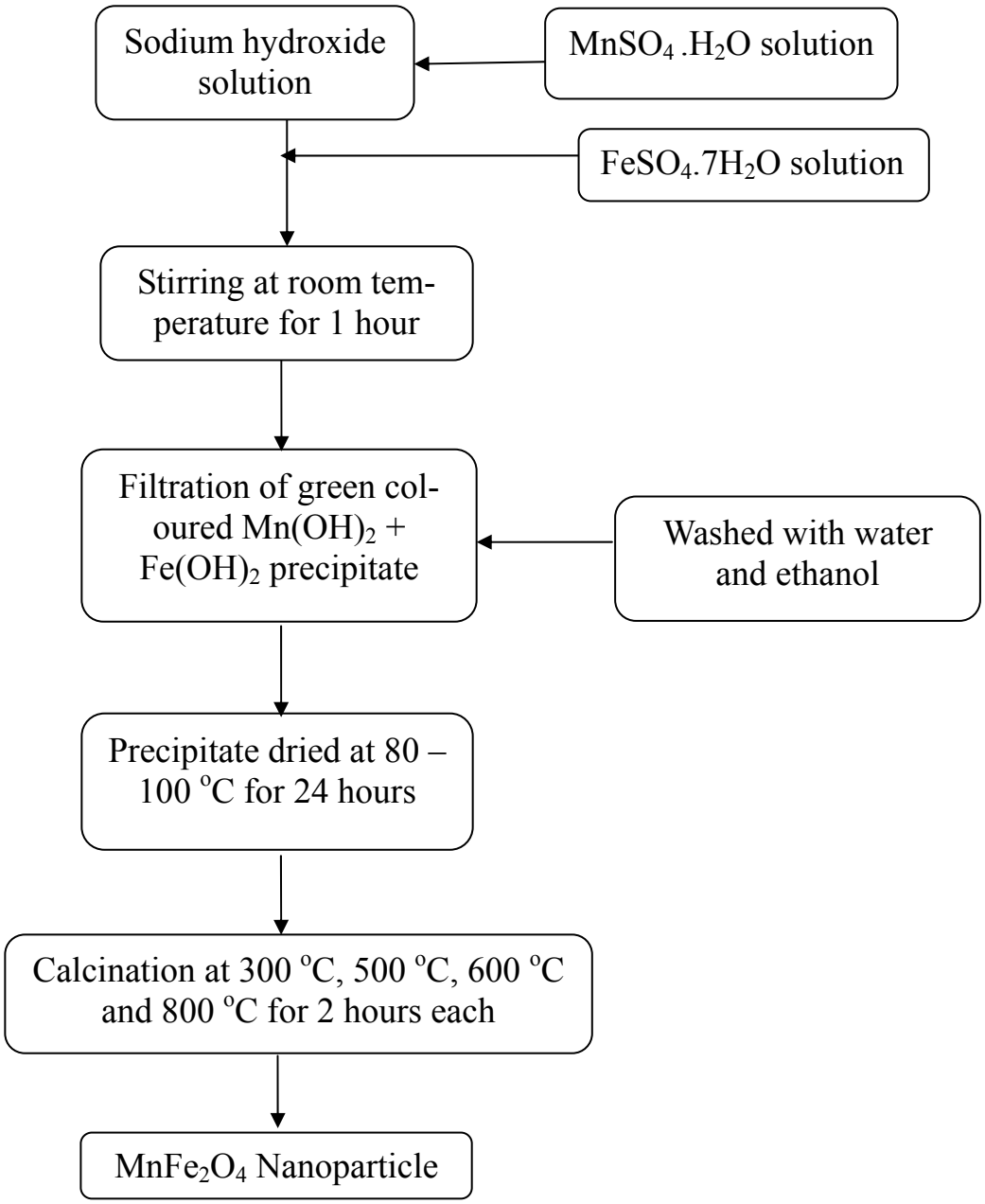

Figure 2. Schematic illustration of the synthesis of $MnFe_2O_4$ nanoparticle by co-precipitation method

3. Results and Discussion

3.1. Structure from powder X-ray diffraction

3.1.1. $MnFe_2O_4$ derived from combustion technique using urea as a fuel

Figure 3 shows the XRD pattern obtain on $MnFe_2O_4$ powder prepared by combustion technique using urea as a fuel, which is indexed to the cubic (f.c.) geometry. The XRD pattern of $MnFe_2O_4$ is compared with standard JCPDS data (card No. 74-2403). Gas-

parov et al. [19] studied the structure of $MnFe_2O_4$ and reported that it has the spinel-type structure. The 2θ values of the combustion derived $MnFe_2O_4$ sample were compared with the above standard JCPDS data. From this, it was found most of the peaks are similar to those of reported pattern of $MnFe_2O_4$ existing in JCPDS card No. 74-2403. Three peaks appeared at $2\theta = 22.30^o$, 70.10^o and 78.90^o are due to impurity phases.

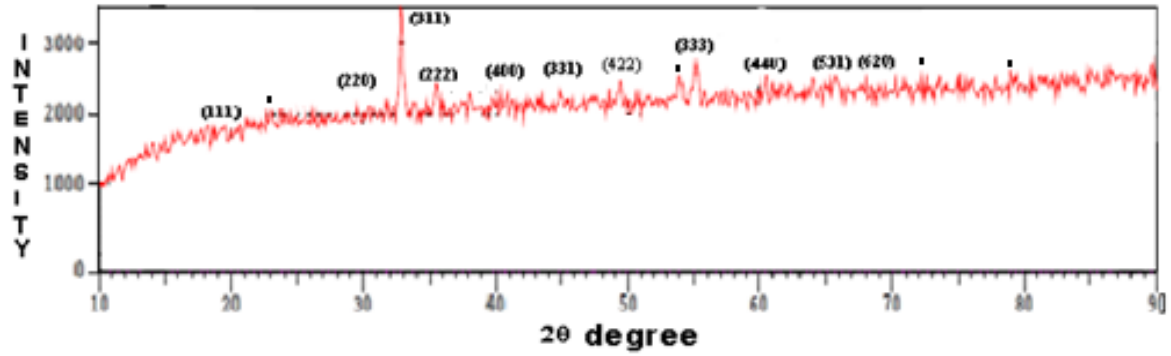

Figure 3. X-ray diffraction pattern obtained on $MnFe_2O_4$ powder synthesized by combustion technique using urea as a fuel

3.1.2. $MnFe_2O_4$ derived from combustion technique using glycine as a fuel

Figure 4 shows the XRD pattern obtain on $MnFe_2O_4$ powder prepared by combustion technique using glycine as a fuel, which is indexed to the cubic cell geometry. The XRD pattern of $MnFe_2O_4$ is compared with standard JCPDS data (card No. 74-2403). From this, it was found that all the peaks are similar to those of reported pattern of $MnFe_2O_4$ existing in JCPDS card No. 74-2403 except two peaks appeared at $2\theta = 22.0551^o$ and 34.92^o. Also, it was found the structure is similar to those of prepared with urea fuel.

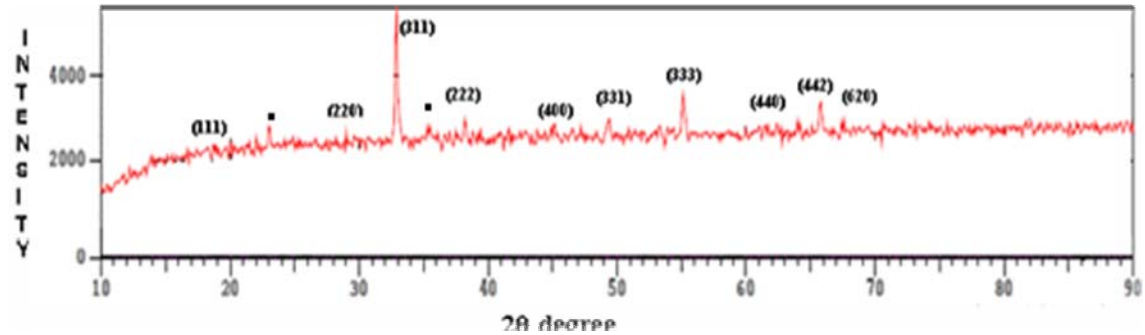

Figure 4. X-ray diffraction pattern obtained on $MnFe_2O_4$ powder synthesized by combustion technique using glycine as a fuel

3.1.3. $MnFe_2O_4$ derived from combustion technique using glucose as a fuel

Figure 5 shows the XRD pattern obtain on $MnFe_2O_4$ powder prepared by combustion technique using glucose as a fuel, which is identified as cubic (f.c.) geometry. The XRD pattern of $MnFe_2O_4$ is compared with standard JCPDS data (card No. 74-2403). From this, it was found that most of the peaks

are similar to those of reported pattern of $MnFe_2O_4$ existing in JCPDS card No. 74-2403. In this sample also, few impurity peaks are appeared at $2\theta = 23.5875^o$, 27.2531^o, 43.18^o and 59.9803^o.

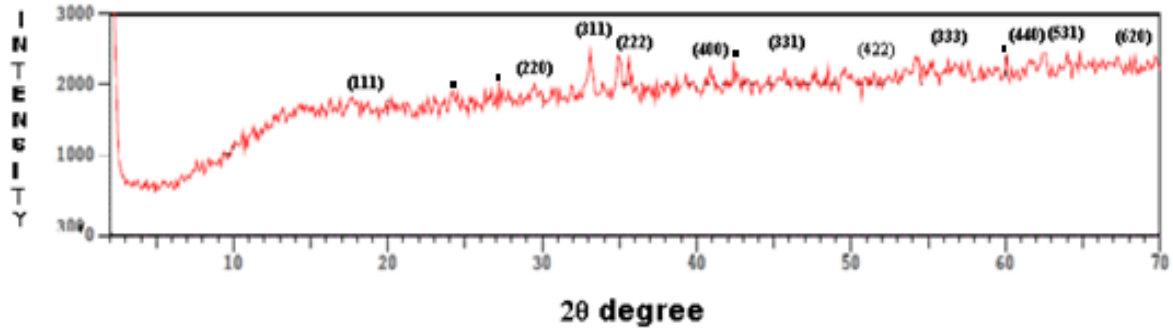

Figure 5. X-ray diffraction pattern obtained on $MnFe_2O_4$ powder synthesized by combustion technique using glucose as a fuel

3.1.4. $MnFe_2O_4$ derived from co-precipitation method

Figure 6 shows the XRD pattern obtain on $MnFe_2O_4$ powder prepared by co-precipitation process, which is indexed to the cubic (f.c.) geometry. The XRD pattern of $MnFe_2O_4$ is compared with standard JCPDS data (card No. 74-2403). From this, it was found all the peaks are similar to those of reported pattern of $MnFe_2O_4$ existing in JCPDS card No. 74-2403 exce-pt three impurity peaks at 22.1000^o, 23.9275^o and 57.3000^o. The impurity peaks appeared in all the samples are found to be the presence of oxides of Mn / Fe as reported [20].

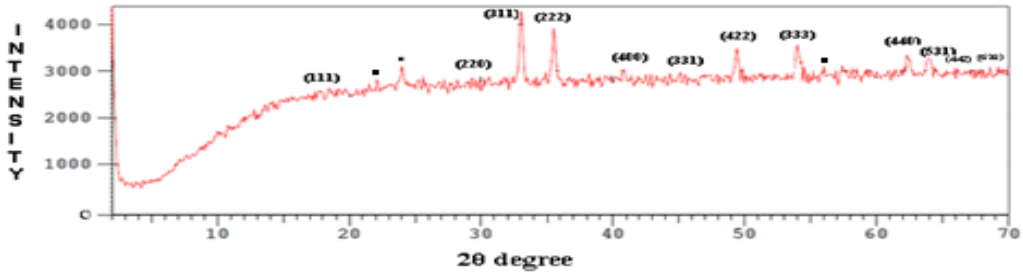

Figure 6. X-ray diffraction pattern obtained on $MnFe_2O_4$ powder synthesized co-precipitation method

3.1.5. Calculation of crystallographic parameters

Lattice parameter (a) for all the samples was calculated by the following lattice parameter formula.

$$a = \frac{d}{(h^2 + k^2 + l^2)^{1/2}}$$

Where 'a' refers to the cubic (f.c.) lattice parameter, and h, k, l are the crystalline face indexes while 'd' is the crystalline face space. $MnFe_2O_4$ particles prepared by different methodologies had exhibited cubic (f.c.)cell geometry as reported [12, 15]. The unit cell volumes calculated for the $MnFe_2O_4$ particles remained uniform. Theoretical or X-ray density (D_{th}) has been calculated (in gcm^{-3}) using the lattice parameters with the formula [21]:

$$D_{th} = z \frac{M}{N \times V}$$

Where 'M' (in atomic-weight units) is the mass of atomic ensemble constituting one unit of the chemical formula, 'z' is the number of such chemical units in one unit cell of the crystal, 'N' is the Avagadro's number (6.022×10^{23} mol^{-1}) and 'V' (in $Å^3$) is the volume of the crystalline unit cell as determined by X-ray diffraction.

The crystallite size of the powder can be calculated from the X-ray diffraction peak intensity analysis using the Scherror formula [22]:

$$x = \frac{0.9\,\lambda}{\beta \cos\theta}$$

where 'x' is crystallite size in nm, 'λ' is the radiation wavelength (for CuKα radiation, λ = 1.5418 Å), 'θ' is the diffraction peak angle and 'β' is the broadening of the line ("half width") measured at half its maximum intensity (in radians).

The crystallographic data obtained on $MnFe_2O_4$ is presented in Table 2. From this, it was understood that the observed unit cell parameter (=a) for all the samples are in agreement with the reported JCPDS data. There is no clear trend observed from the observed unit cell volumes and theoretical density data. However, the values are almost similar. The crystalline size values ranges between 11 – 15 nm. The mean crystallite size of the $MnFe_2O_4$ is reported as 13.2 nm [23] prepared by solution method. Hence, the crystallite size values of our samples are in accordance with the data reported earlier.

Table 2. Crystallographic properties obtained on $MnFe_2O_4$ powder

Process	Crystal structure	Unit Cell parameter-'a' (Å)	Unit cell volume ($Å^3$)	Theoretical density (g/cc)	Crystallite size (nm)
$MnFe_2O_4$ Powder (JCPDS No. 74-2403)	Cubic (f.c.)	8.511	616.5123	2.4843	--
Urea process	Cubic (f.c.)	8.5103	616.36023	2.4849	15.4885
Glycine process	Cubic (f.c.)	8.5191	618.2742	2.4773	15.4885
Glucose process	Cubic (f.c.)	8.5253	618.3831	2.4875	11.6157
Co-precipitation	Cubic (f.c.)	8.4698	633.9061	2.4161	14.1046

3.2. Particulate properties of $MnFe_2O_4$ powder

The prepared $MnFe_2O_4$ particles (after calcination at 800 ^oC for 3 h) were subjected to particle size measurements using Malvern particle size anlyzer with triple distilled water as medium. For all the measurements, 0.30 g of sample is sonicated in 30 ml triple distilled water for about 10 minutes and after that the sample is subjected for particle size analysis. The particle size distribution curves of $MnFe_2O_4$ are shown in Figure 7-14.

3.2.1. Particle size distribution data of $MnFe_2O_4$ prepared by combustion technique using urea as a fuel

The particle size distribution curves obtained with $MnFe_2O_4$ prepared by combustion with urea as a fuel is shown in Figure 7 and 8. From the particle characteristics (based on intensity) data, it was understood that 51.5 % of particles are present below 389.1 nm and remaining 44.9 % particles are present below 4.917 µm. From the particle characteristics (based on volume) data, it was understood that 4.3 % of particles are present below 405.6 nm and 95.7 % of particle are present below 5.083 µm. The average particle size of $MnFe_2O_4$ particles prepared by combustion technique using urea as a fuel is found to be 899.8 d.nm. The particle characteristics data revealed that the $MnFe_2O_4$ particles prepared by combustion technique using urea as a fuel are present in micron size range.

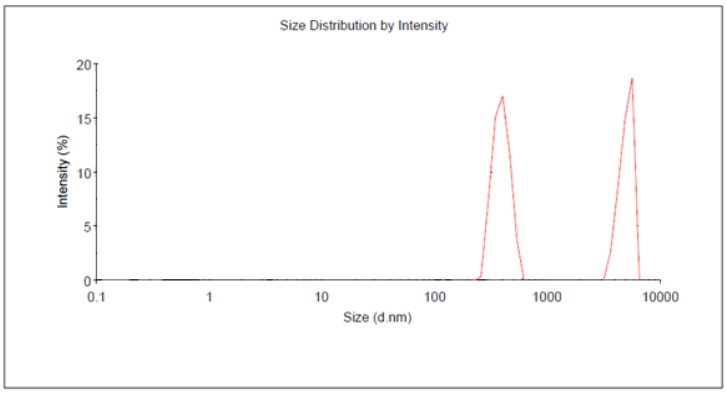

Figure 7. Particle size distribution pattern (based on intensity) obtained on $MnFe_2O_4$ prepared by combustion method using urea as a fuel

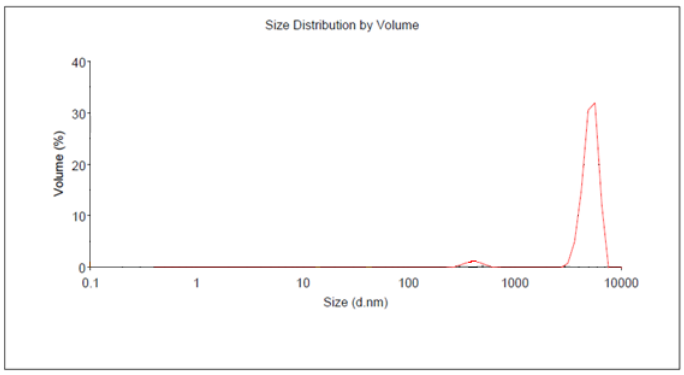

Figure 8. Particle size distribution pattern (based on volume) obtained on $MnFe_2O_4$ prepared by combustion method using urea as a fuel

3.2.2. Particle size distribution data of $MnFe_2O_4$ prepared by combustion technique using glycine as a fuel

The particle size distribution curves obtained with $MnFe_2O_4$ prepared by combustion with glycine as a fuel is shown in Figure 9 and 10. From the particle characteristics (based on intensity) data, it was understood that 66.6 % of particles are present below 3.889 μm and remaining 33.4 % particles are present below 243 nm. From the particle characteristics (based on volume) data, it was understood that 98.4 % of particles are present below 4.337 μm and 1.6 % of particle are present below 248.9 nm. The average particle size of $MnFe_2O_4$ particles prepared by combustion technique using glycine as a fuel is found to be 800.4 d.nm. From the particle characteristics data, it was found that the $MnFe_2O_4$ prepared by combustion technique using glycine as a fuel has lower average particle size than the sample prepared with combustion technique using urea as a fuel.

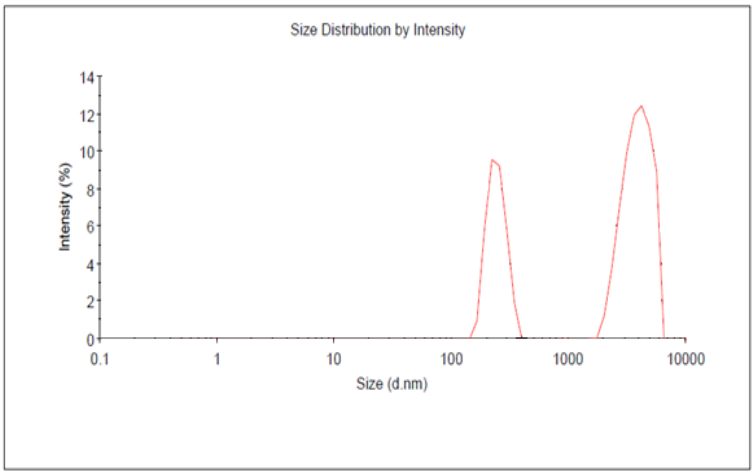

Figure 9. Particle size distribution pattern (based on intensity) obtained on $MnFe_2O_4$ prepared by combustion method using glycine as a fuel

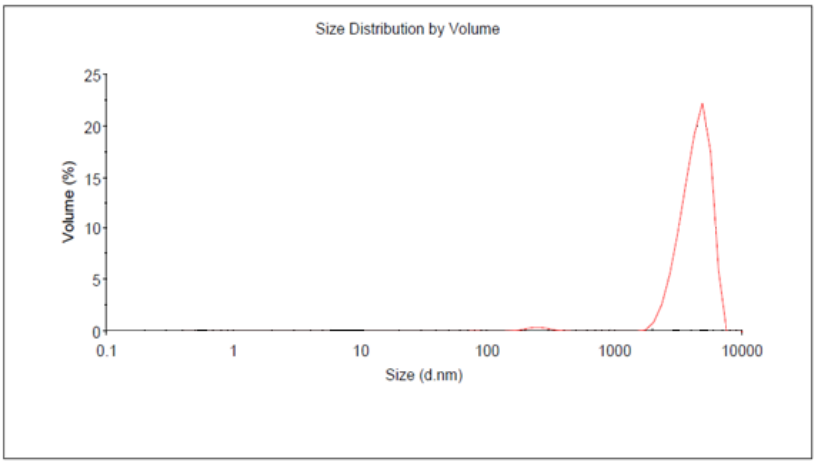

Figure 10. Particle size distribution pattern (based on volume) obtained on $MnFe_2O_4$ prepared by combustion method using glycine as a fuel

3.2.3. Particle size distribution data of $MnFe_2O_4$ prepared by combustion technique using glucose as a fuel

The particle size distribution curves obtained with $MnFe_2O_4$ prepared by combustion with glucose as a fuel is shown in Figures 11 and 12. From the particle characteristics (based on intensity) data, it was understood that 56.2 % of particles are present below 4.237 μm and remaining 43.8 % particles are present below 294.9 nm. From the particle characteristics (based on volume) data, it was understood that 97.5 % of particles are present below 4.550 μm and 2.5 % of particle are present below 306.1 nm.

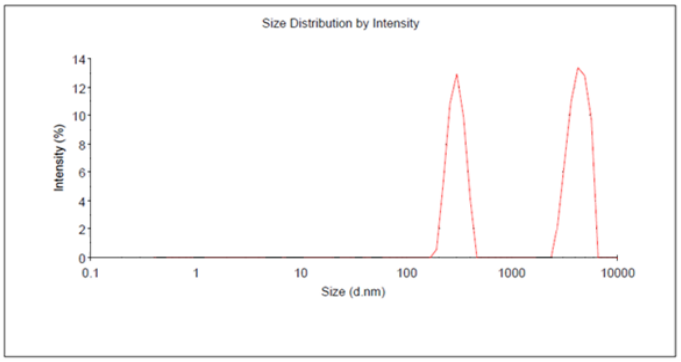

Figure 11. Particle size distribution pattern (based on intensity) obtained on $MnFe_2O_4$ prepared by combustion method using glucose as a fuel

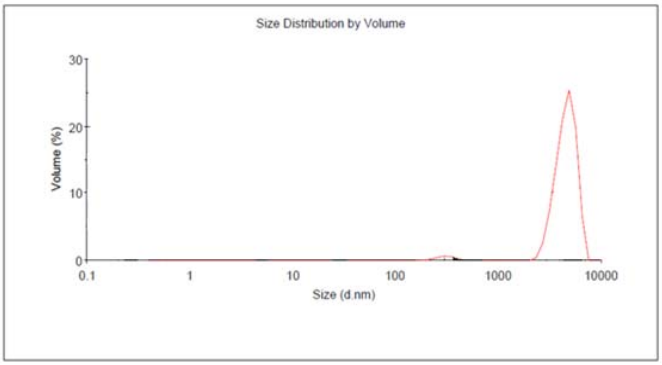

Figure 12. Particle size distribution pattern (based on volume) obtained on $MnFe_2O_4$ prepared by combustion method using glucose as a fuel

The average particle size of $MnFe_2O_4$ particles prepared by combustion technique using glucose as a fuel is found to be 661.9 d.nm. From the particle characteristics data, it was found that the $MnFe_2O_4$ prepared by combustion technique using glucose as a fuel has lower average particle size than the samples prepared with combustion technique using urea and glycine as a fuels. The lower particle size of the sample prepared with glucose may be due to the liberation of large moles of gases during synthesis (Please refer to the reported combustion reaction mentioned earlier for the preparation $MnFe_2O_4$ using glucose as a fuel)[24].

3.2.4. Particle size distribution data of $MnFe_2O_4$ prepared by co-precipitation process

The particle size distribution curves obtained with $MnFe_2O_4$ prepared by co-precipitation process is shown in Figure 13 and 14. From the particle characteristics (based on intensity) data, it was understood that 57.2 % of particles are present below 4.608 μm and remaining 42.8 % particles are present below 229 nm.From the particle characteristics (based on volume) data, it was understood that 98.1 % of particles are present below 4.849 μm and 1.9 % of particle are present 232.1 nm. The average particle size of $MnFe_2O_4$ particles prepared by co-precipitation method is 603.6 d.nm. From the particle characteristics data, it was understood that the particles prepared with chemical precipitation method exhibited very low particle size.

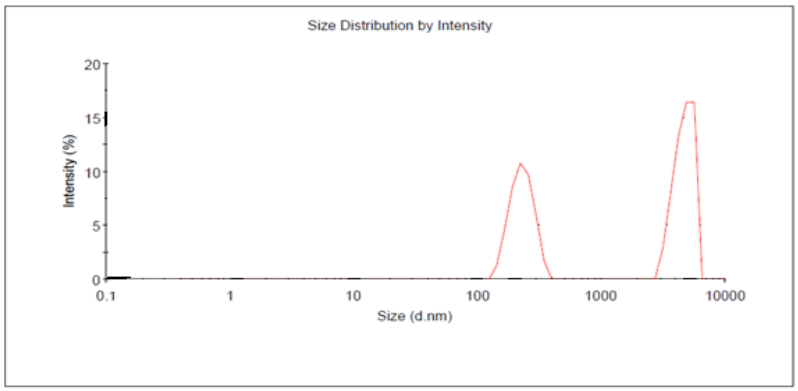

Figure 13. Particle size distribution pattern (based on intensity) obtained on $MnFe_2O_4$ prepared by co-precipitation method

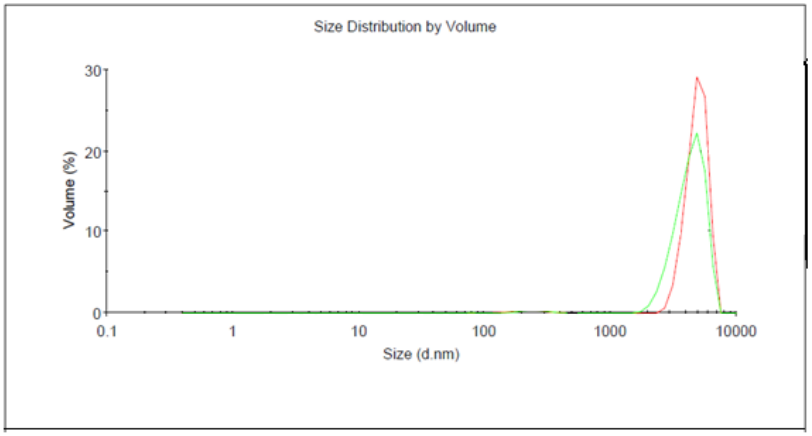

Figure 14. Particle size distribution pattern (based on volume) obtained on $MnFe_2O_4$ prepared by

3.3. Scanning Electron Microscopic (SEM) studies of $MnFe_2O_4$ powder

The surface microstructure of $MnFe_2O_4$ was studied with SEM. The arrangement of grains, size of grains, etc. were differed for the samples based on the preparative conditions.

3.3.1. SEM studies obtained on $MnFe_2O_4$ prepared with urea as a fuel

Figure 15 shows the microstructure of $MnFe_2O_4$ prepared by combustion technique using urea as a fuel. From the SEM photographs, it was understood that the sample consisting of grains with average size of 200-300 nm. The grains are connected with each other. In few places, bigger grains (800 nm) are also seen.

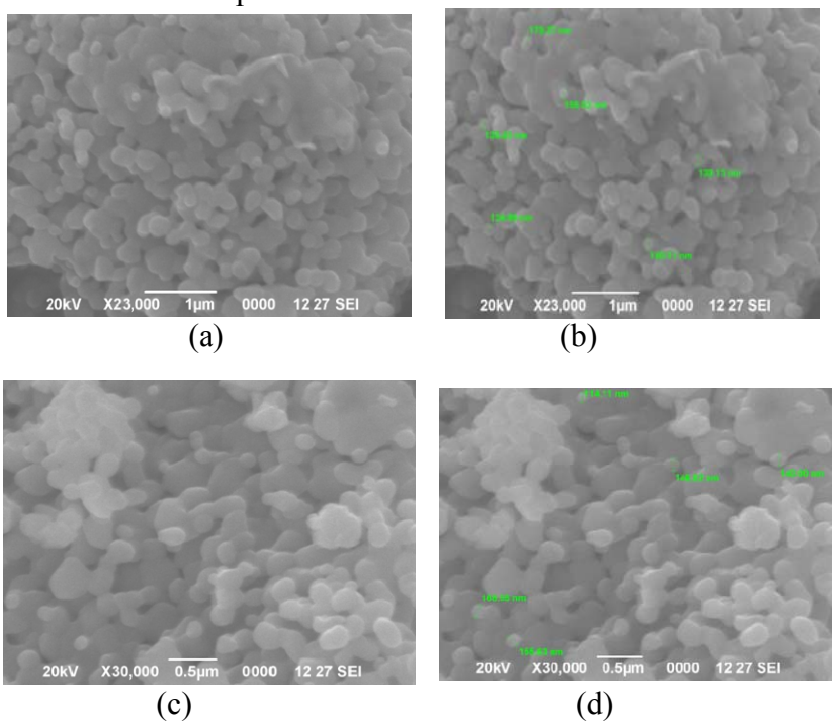

Figure 15. SEM photographs obtained on $MnFe_2O_4$ synthesized by combustion technique using urea as a fuel

3.3.2. SEM studies obtained on $MnFe_2O_4$ prepared with glycine as a fuel

Figure 16 shows the microstructure of $MnFe_2O_4$ prepared by combustion technique using glycine as a fuel. From the SEM photographs, it was understood that the sample consisting of grains with average size of 200 nm. Inter connected grains are also present in the samples. It was understood that $MnFe_2O_4$ powder synthesized through combustion synthesis using glycine as the fuel gives clustered porous structure.

3.3.3. SEM studies obtained on MnFe2O4 prepared with glucose as a fuel

Figure 17 shows the microstructure of MnFe2O4 prepared by combustion technique using glucose as a fuel. From the SEM photographs, it was understood that the sample consisting of grains with average size of 2 - 3 µm. It was found that the grains are present individually in the powder. The presence of big agglomerates in the powder is due to high temperature calcination.

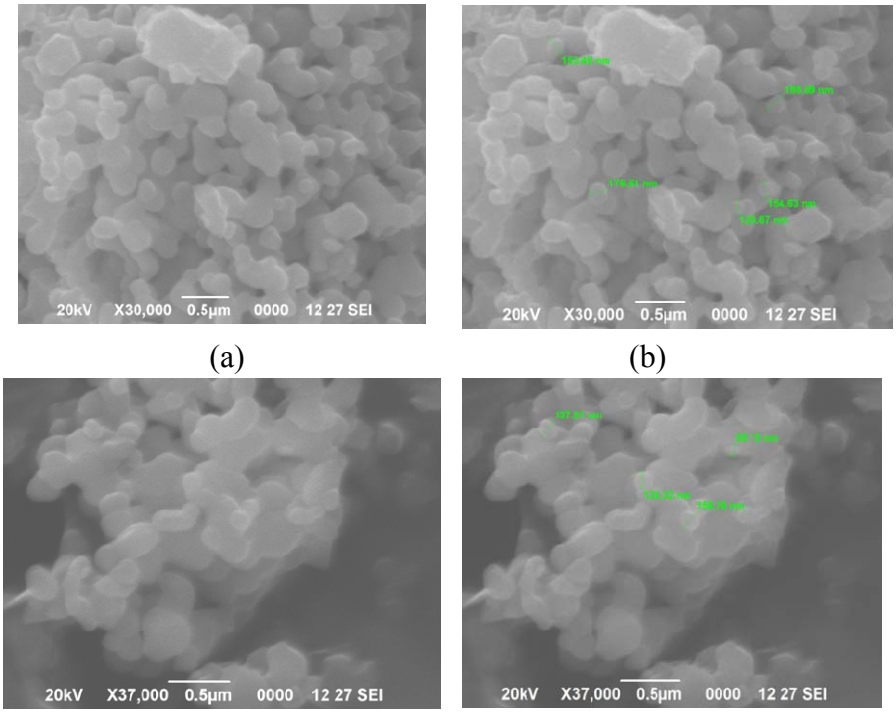

Figure 16. SEM photographs obtained on $MnFe_2O_4$ synthesized by combustion technique using glycine as a fue

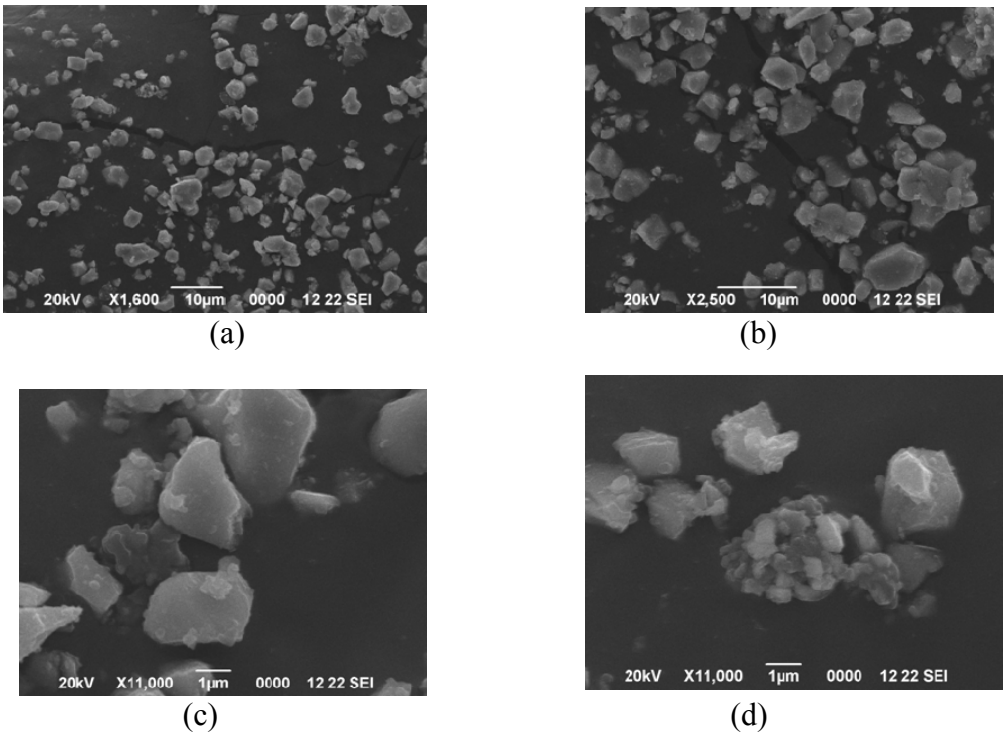

Figure 17. SEM photographs obtained on $MnFe_2O_4$ synthesized by combustion technique using glucose as a fuel

3.3.4. SEM studies obtained on $MnFe_2O_4$ prepared by co-prcipitation method

Figure 18 shows the microstructure of $MnFe_2O_4$ prepared by co-precipitation method. From the SEM photographs, it was understood that the sample consists of grains with average size of 200 nm. It was found that the grains present jointly with each other. It was understood that, $MnFe_2O_4$ sample synthesized through co-precipitation process resulted in very low particle size when compared with the other samples prepared by combustion technique using different fuels.

4. Conclusions

Synthesis of $MnFe_2O_4$ particles by combustion technique and co-precipitation method for application is dealt with. The powder XRD data obtained on $MnFe_2O_4$ powder is in good agreement with the standard reported XRD data except with few impurity phases. From the particle characteristics data and SEM data, it is arrived that the sample prepared with co-precipitation method is found to be shown better particulate properties with more nano sized particles when compared with the samples prepared with other methods.

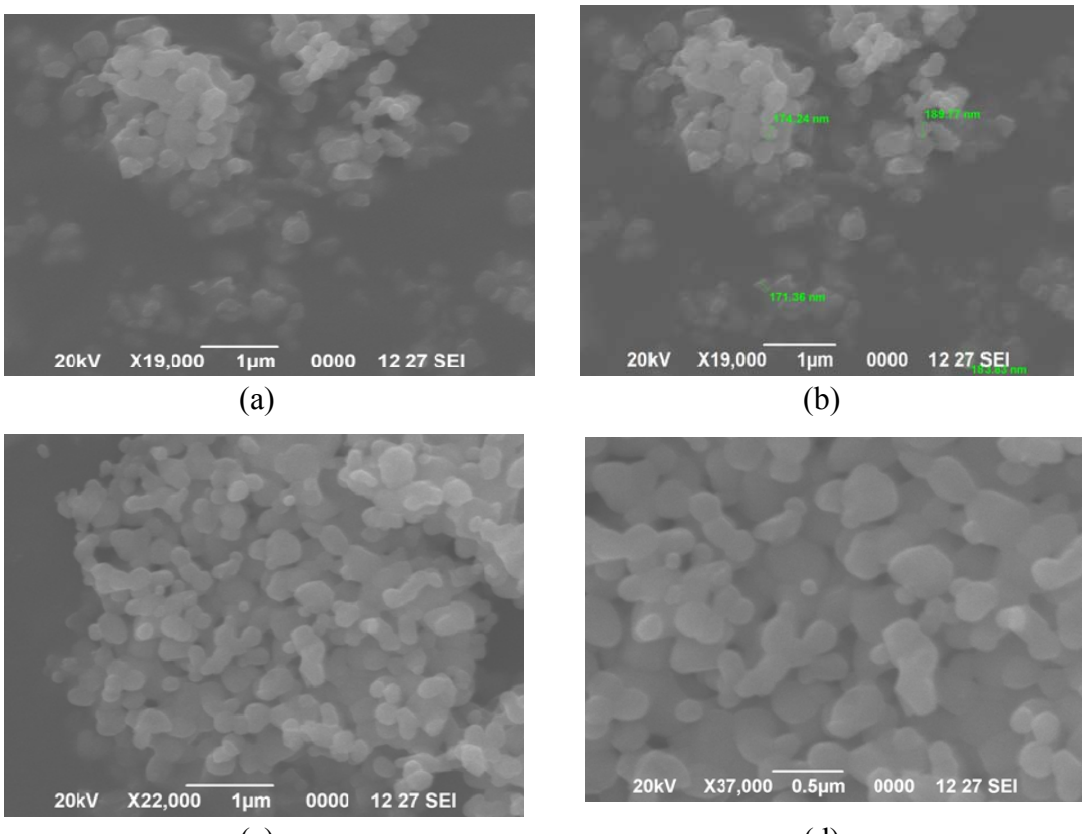

Figure 18. SEM photograph obtained on $MnFe_2O_4$ synthesized prepared by co-precipitation method

Acknowledgement

ASN thanks the Administration of Karunya University for promoting high temperature materials research activity at Karunya University

References

[1] Zuo, X., Yang, A., Yoon, S., Christodoulides, J., Harris, V. G., and Vittoria, C. 2005. Large induced magnetic anisotropy in manganese spinel ferrite films. *Applied Physics Lett*ers, 87, 15: 2505-2507.

[2] Ang, K. L., Venkatraman, S., and Ramanujan, R. V. 2007. Magnetic PNIPA hydrogels for hyperthermia applications in cancer therapy. *Materials Science and Engineering: C*, 27: 347-351.

[3] Wu, R., and Qu, J. 2005. Removal of water-soluble azo dye by the magnetic material $MnFe_2O_4$. *Journal of Chemical Technology and Biotechnology*, 80: 20-27.

[4] Ahmed, M. A., Okasha, N., and El-Dek, S. I. 2008. Preparation and characterization of nanometric Mn ferrite via different methods. *Nanotechnology*, 19: 1-6.

[5] Amighian, J., Mozaffer, M., and Nasr, B. 2006. Preparation of nano-sized manganese ferrite ($MnFe_2O_4$) via coprecipitation method. *Physica Status Solidi. C. Current Topics in Solid State Physics*, 3: 3188-3192.

[6] Solis,T. V., Vigon, P. V., Alvarez, S., Marban, G., and Fuertes, A. B. 2007. Manganese ferrite nanoparticles synthesized through a nanocasting route as a highly active Fenton catalyst. *Catalysis Communication*, 8: 2037-2042.

[7] Mishra, S., Kundu, T. K., Barick K. C., and Bahadur, D. 2006. Preparation of nanocrystalline $MnFe_2O_4$ by doping with Ti^{4+} ions using solid-state reaction route. *Journal of Magnetism and Magnetic Materials*, 307: 222-226.

[8] Rashad, M. M. 2006. Synthesis and magnetic properties of manganese ferrite from low grade manganese ore, *Materials Science Engineering: B*, 127: 123-129.

[9] Yang, H., Zhang, C., Shi, X., Hu, H., Du, X., Fang, Y., Ma, Y., Wu, H., and Yang, S. 2010. Water-soluble superparamagnetic manganese ferrite nanoparticles for magnetic resonance imaging. *Biomaterials*, 31: 3667-3673.

[10] Choi, H. N., Baek, K. S., Hyun, S. W., Shim, I. B., and Kim, C. S. 2009. A Study of Co Substituted Mn-Ferrite, $Mn_{1-x}Co_xFe_2O_4$(x = 0.0,0.5,1.). *IEEE Transactions on Magnetics*, 45: 2554-2556.

[11] Rucha, D., Vipul, D., Kinnari, P., and Ramesh, V. U. 2009. Structural and magnetic properties of size-controlled $Mn_{0.5}Zn_{0.5}Fe_2O_4$ nanoparticles and magnetic fluids. *Pramana Journal of Physics*, 73: 765-780.

[12] Iyer, R., Desai, R., and Upadhayay, R. V. 2009. Low temperature synthesis of nanosized $Mn_{1-x}Zn_xFe_2O_4$ ferrites and their characterizations. *Bulletin Materials Science*, 32: 141-147.

[13] Deraz, N. M., and Shaban, S. 2009. Optimization of Catalytic, Surface and Magnetic Properties of Nanocrystalline Manganese Ferrite. *Journal Analytical and Applied Pyrolysis*, 86: 173-179.

[14] Ju, Y. W., Park, J. H., Jung, H. R., Cho, S. J., and Lee, W. J. 2008. Electrospun $MnFe_2O_4$ nanofibers: Preparation and morphology. *Composites Science and Technology*, 68: 1704-1709.

[15] Kim, J. G., Seo, J. W., Cheon, J., and Kim, Y. J. 2009. Rietweld Analysis of Nano-crystalline $MnFe_2O_4$ with Electron Powder Diffraction. *Bulletin of Korean Chemical Society,* 30: 183-187.

[16] Arul Dhas, N., and Patil, K. C. 1993. Properties of magnesia-stabilized zirconia powders prepared by a combustion route. *Journal of Materials Science Letters*, 12: 1844-1847.

[17] Farh, L. E., Massot, M., Lemal, M., Julien, C., Chitra, S., Kalyani, P., Mohan, T., and Gangadharan, R. 1999. Physical Properties and Electrochemical Features of Lithium Nickel-Cobalt Oxide Cathode Materials Prepared at Moderate Temperature. *Journal of Electroceramics*, 3-4: 425-432.

[18] Hatchwell, C., Sammes, N. M., Brown, I. W. M., and Kendall, K. 1999. Current collectors for a novel tubular. SOFC design. *Journal of Power Sources*, 77: 64-68.

[19] Gasparov, L., Rush, A., Pekarek, T. Patel, N., and Helmuth, B. 2009. Raman studies of doped magnetite above and below the Verwey transition. *Journal of Applied Physics*, 105, 7: 07E109-07E109-3.

[20] Osmokrovic, P., Jovalekic, C., Manojlovic, D., and Pavlovic, M. B. 2006. Synthesis of $MnFe_2O_4$ nanoparticles by mechanochemical reaction. *Journal of Optoelectronics and Advanced Materials*, 8: 312-314.

[21] Kostogloudis, G. Ch., Vasilakos, N., and Ftikos, Ch. 1997. $Pr_{1-x}Sr_xMnO_{3\pm\delta}$ (x = 0, 0.15, 0.3, 0.4, 0.5) as a Potential SOFC Cathode Material Operating at Intermediate Temperatures (500-700 °C). *Journal of European Ceramic Society*, 17: 1513-1521.

[22] Shaji Kumar, M. D., Srinivasan, T.M., Ramasamy P., and Subramanian, C. 1994. Synthesis of lanthanum aluminate by a citrate-combustion route. *Materials Letters*, 25, 3-4: 171-174.

[23] Kuo, S. L., and Wu, N. L. 2005. Electrochemical Capacitor of $MnFe_2O_4$ with NaCl

[24] Chavan, S. V., Pillai. K. T., and Tyagi, A. K. 2006. Combustion synthesis of nanocrystalline yttria: Tailoring of powder properties. *Materials Science and Materials and Engineering B*, 132: 266-271